

# Multiply inner-shell excited states produced through multiple x-ray absorption relevant to x-ray pulses

Kengo Moribayashi\*

*Japan Atomic Energy Agency, 8-1, Umemidai, Kizu-cho, Kyoto, 619-0215, Japan*

(Received 8 February 2007; revised manuscript received 11 June 2007; published 8 October 2007)

We study fluorescence x rays emitted from multiply inner-shell excited states produced by high-brightness x-ray absorption. The pulses of the fluorescence x rays from the multiply inner-shell excited states are shorter than that of the original x-ray source. As the pulse of x-ray sources becomes shorter, hollow atoms are produced more efficiently.

DOI: [10.1103/PhysRevA.76.042705](https://doi.org/10.1103/PhysRevA.76.042705)

PACS number(s): 32.80.Hd, 32.80.Fb, 41.50.+h

## I. INTRODUCTION

High-brightness short-pulse ( $\sim 100$  fs) x-ray free-electron laser (XFEL) sources will be developed as high-energy probes of matter in the United States, European Union, and Japan around 2010 [1,2]. Such x-ray sources have also been developed as laser-driven x-ray sources [3–7]. These high-brightness short-pulse x-ray sources are expected to measure the structure of biological materials without crystallization [8,9]. However, since high-brightness x rays damage the target materials, shorter x-ray pulses, which can measure the targets with little damage, are desirable [8,9]. For example, the required x-ray pulse is calculated to be smaller than 5 fs for atom length structural measurement of proteins [8]. These x-ray sources are also useful for (1) the measurement of ultrafast processes such as those occurring in material science [10,11], the photoreceptors of our eyes [12,13], and photosynthesis [14,15] and (2), the production of photoionized plasma [16,17].

Inner-shell excited states produced by x-ray absorption are useful for the measurement of materials. For example, the spectra of Auger electrons have been used for structural measurements of materials [18]. Furthermore, by using the fluorescence x-ray holography method, the cubic structures of materials have been measured [19,20]. By using high-brightness short-pulse x rays, these techniques may also be applied to the structural measurement of biological materials.

Moribayashi *et al.* found a new characteristic in the production of multiply inner-shell excited states by high-brightness x rays [21–23]. They devised an x-ray laser scheme using hollow atoms, which originate from inner-shell ionization x-ray lasers pumped by very high-brightness x rays [21]. In this case, inner-shell ionization processes become much faster than any other atomic processes, such as autoionization and radiation transition processes. As a result, multiply inner-shell ionizations predominate, leading to the formation of multiply inner-shell excited states, or hollow atoms. In contrast, for an ordinary x-ray source, since autoionization or radiation transition processes are much faster than photoionization processes, further inner-shell ionizations from inner-shell excited states seldom occur. From this characteristic, they showed that x-ray emissions from hollow

atoms give information about the x-ray intensities of high-irradiance x-ray sources [22]. Furthermore, they proposed measurement of the pulses of femtosecond pulse x rays by using fluorescence x rays from multiply inner-shell excited states and an autocorrelation method [23].

In this paper, we study (i) x-ray pulses emitted from multiply inner-shell excited states produced by high-brightness x rays vs the pulse of the original x ray and (ii) the production ratio of multiply inner-shell excited states as a function of the x-ray pulses and irradiances of the original x-ray source. This may be useful for the measurement of structure using an XFEL, for instance, using fluorescence x-ray spectra [18] or fluorescence x-ray holography [19,20] to understand the characteristics of multiply inner-shell excited states produced through multiple-x-ray absorption.

## II. METHOD OF CALCULATION

The methods of calculation and the model employed here are the same as those in Refs. [21–23]. Here, we treat argon atoms as the target material. Argon is a good target material for the first demonstration experiment because it is easy to treat as a gas or clusters. We employ x-ray absorption ionization ( $A_i$ ), radiative transition ( $A_r$ ), and autoionization ( $A_a$ ) processes. For example, in the case of the ground state of argon atoms ( $1s^2 2s^2 2p^6 3s^2 3p^6$ ), the following processes are considered:

$$\text{Ar}(1s^2 2s^2 2p^6 3s^2 3p^6) + h\nu \rightarrow \text{Ar}^+(1s^2 2s^2 2p^6 3s^2 3p^5) + e^-, \quad (1)$$

$$\text{Ar}(1s^2 2s^2 2p^6 3s^2 3p^6) + h\nu \rightarrow \text{Ar}^+(1s^2 2s^2 2p^6 2p^6 3s^2 3p^6) + e^-, \quad (2)$$

$$\text{Ar}(1s^2 2s^2 2p^6 3s^2 3p^6) + h\nu \rightarrow \text{Ar}^+(1s^2 2s^2 2p^5 3s^2 3p^6) + e^-, \quad (3)$$

$$\text{Ar}(1s^2 2s^2 2p^6 3s^2 3p^6) + h\nu \rightarrow \text{Ar}^+(1s^2 2s 2p^6 3s^2 3p^6) + e^-. \quad (4)$$

On the other hand, from the inner-shell excited states of argon, the  $A_r$  and  $A_a$  processes are given by

$$\text{Ar}^+(1s^2 2s^2 2p^5 3s^2 3p^6) \rightarrow \text{Ar}^+(1s^2 2s^2 2p^6 3s^2 3p^6) + h\nu [A_r(3s - 2p)], \quad (5)$$

\*FAX: +81-774-71-3316. moribayashi.kengo@jaea.go.jp

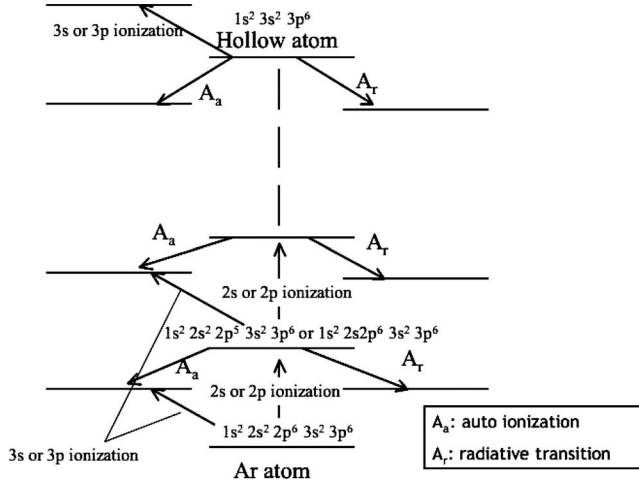
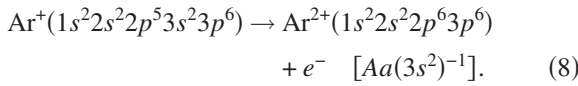
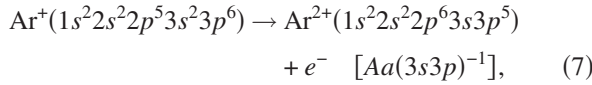
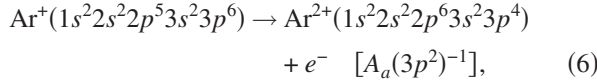


FIG. 1. Atomic processes relevant to multiple-x-ray ionization such as photoionization, autoionization, and radiative transition (see Table I for autoionization and radiative transition).



We ignore the electron impact ionization processes because we assume a gas target with low density ( $<10^{19}/\text{cm}^3$ ). The atomic data employed here are calculated by using Cowan's code [24]. Figure 1 shows the atomic processes relevant to multiply inner-shell ionizations, such as photoionization, autoionization, and radiative transitions. The detailed atomic processes for autoionization, and radiative transitions are listed in Table I. With these atomic processes, the population dynamics of the various atomic states may be investigated using the rate equations, that is,

$$\frac{dP_0}{dt} = -\beta_0 P_0,$$

$$\frac{dP_1}{dt} = \alpha_{0,1} P_0 - \beta_1 P_1,$$

⋮

$$\frac{dP_h}{dt} = \alpha_{n,h} P_n - \beta_h P_h, \quad (9)$$

where  $P_0, P_1, P_2, \dots, P_h$  are the populations of the ground state, the inner-shell excited state, the doubly inner-shell excited state, and soon, and the hollow atoms of Ar, respectively,  $\alpha_{m,k}$  is the transition rate via the inner-shell photoionization processes from the  $m$ th to the  $k$ th state, and  $\beta_k$  is the

TABLE I. Atomic data for argon. (a)  $E_{\text{av}}$  and  $A_r$ . For the calculation, Eqs. (11) and (12) are used. The first to fourth columns list the transition number, initial and final states,  $E_{\text{av}}$ , and  $A_r$ . For the transition, the initial and final states for  $n=2$  are shown. (b)  $A_a$ . For the calculation, Eq. (12) is used. The first column lists the initial and final states for  $n=2$ , and the second to fourth columns give  $A_a$  for final states of  $n=3$ .

No.	States	$E_{\text{av}}$ (eV)	$A_r$ (1/s)
(a)			
1	$2s^2 2p^5 - 2s^2 2p^6$	215	$4.47 \times 10^{10}$
2	$2s^2 2p^4 - 2s^2 2p^5$	241	$1.11 \times 10^{11}$
3	$2s^2 2p^3 - 2s^2 2p^4$	268	$2.00 \times 10^{11}$
4	$2s^2 2p^2 - 2s^2 2p^3$	298	$3.14 \times 10^{11}$
5	$2s^2 2p - 2s^2 2p$	330	$4.55 \times 10^{11}$
6	$2s^2 - 2s^2 2p$	362	$6.22 \times 10^{11}$
7	$2s 2p^5 - 2s 2p^6$	237	$5.13 \times 10^{10}$
8	$2s 2p^4 - 2s 2p^5$	262	$1.24 \times 10^{11}$
9	$2s 2p^3 - 2s 2p^4$	290	$2.19 \times 10^{11}$
10	$2s 2p^2 - 2s 2p^3$	320	$3.38 \times 10^{11}$
11	$2s 2p - 2s 2p^2$	352	$4.82 \times 10^{11}$
12	$2s - 2s 2p$	385	$6.50 \times 10^{11}$
13	$2p^5 - 2p^6$	256	$5.65 \times 10^{10}$
14	$2p^4 - 2p^5$	283	$1.34 \times 10^{11}$
15	$2p^3 - 2p^4$	314	$2.33 \times 10^{11}$
16	$2p^2 - 2p^3$	345	$3.54 \times 10^{11}$
17	$2p - 2p^2$	378	$4.97 \times 10^{11}$
18	Hollow atom-2p	413	$6.63 \times 10^{11}$
19	$2s 2p^6 - 2s^2 2p^6$	312	$4.46 \times 10^{11}$
20	$2s 2p^5 - 2s^2 2p^5$	333	$6.31 \times 10^{11}$
21	$2s 2p^4 - 2s^2 2p^4$	354	$8.55 \times 10^{11}$
22	$2s 2p^3 - 2s^2 2p^3$	377	$1.12 \times 10^{12}$
23	$2s 2p^2 - 2s^2 2p^2$	400	$1.43 \times 10^{12}$
24	$2s 2p - 2s^2 2p$	423	$1.79 \times 10^{12}$
25	$2s - 2s^2$	446	$2.20 \times 10^{12}$
26	$2p^6 - 2s 2p^6$	338	$1.27 \times 10^{12}$
27	$2p^5 - 2s 2p^5$	358	$1.71 \times 10^{12}$
28	$2p^4 - 2s 2p^4$	379	$2.24 \times 10^{12}$
29	$2p^3 - 2s 2p^3$	401	$2.86 \times 10^{12}$
30	$2p^2 - 2s 2p^2$	424	$3.58 \times 10^{12}$
31	$2p - 2s 2p$	448	$4.40 \times 10^{12}$
32	Hollow atom-2s	473	$5.34 \times 10^{12}$
(b)			
States	$A_a$ ( $3s^2 3p^4$ ) (1/s)	$A_a$ ( $3s^3 p^5$ ) (1/s)	$A_a$ ( $3p^6$ ) (1/s)
$2s^2 2p^5 - 2s^2 2p^6$	$1.19 \times 10^{14}$	$3.62 \times 10^{13}$	$1.20 \times 10^{12}$
$2s^2 2p^4 - 2s^2 2p^5$	$3.30 \times 10^{14}$	$9.39 \times 10^{13}$	$3.66 \times 10^{12}$
$2s^2 2p^3 - 2s^2 2p^4$	$6.47 \times 10^{14}$	$1.72 \times 10^{14}$	$7.33 \times 10^{12}$
$2s^2 2p^2 - 2s^2 2p^3$	$1.01 \times 10^{15}$	$2.75 \times 10^{14}$	$1.21 \times 10^{13}$
$2s^2 2p - 2s^2 2p^2$	$1.55 \times 10^{15}$	$3.99 \times 10^{14}$	$1.78 \times 10^{13}$
$2s^2 - 2s^2 2p$	$2.18 \times 10^{15}$	$5.47 \times 10^{14}$	$2.39 \times 10^{13}$

TABLE I. (Continued.)

States	$A_a$ ( $3s^23p^4$ ) (1/s)	$A_a$ ( $3s3p^5$ ) (1/s)	$A_a$ ( $3p^6$ ) (1/s)
$2s2p^5$ - $2s2p^6$	$1.65 \times 10^{14}$	$4.65 \times 10^{13}$	$1.94 \times 10^{12}$
$2s2p^4$ - $2s2p^5$	$4.23 \times 10^{14}$	$1.15 \times 10^{14}$	$5.27 \times 10^{12}$
$2s2p^3$ - $2s2p^4$	$7.85 \times 10^{14}$	$2.06 \times 10^{14}$	$9.72 \times 10^{12}$
$2s2p^2$ - $2s2p^3$	$1.24 \times 10^{15}$	$3.20 \times 10^{14}$	$1.50 \times 10^{13}$
$2s2p$ - $2s2p^2$	$1.79 \times 10^{15}$	$4.52 \times 10^{14}$	$2.09 \times 10^{13}$
$2s$ - $2s2p$	$2.42 \times 10^{15}$	$6.13 \times 10^{14}$	$2.70 \times 10^{13}$
$2p^5$ - $2p^6$	$2.07 \times 10^{14}$	$5.74 \times 10^{13}$	$2.83 \times 10^{12}$
$2p^4$ - $2p^5$	$5.09 \times 10^{14}$	$1.38 \times 10^{14}$	$6.97 \times 10^{12}$
$2p^3$ - $2p^4$	$9.10 \times 10^{14}$	$2.39 \times 10^{14}$	$1.19 \times 10^{13}$
$2p^2$ - $2p^3$	$1.36 \times 10^{15}$	$3.64 \times 10^{14}$	$1.76 \times 10^{13}$
$2p$ - $2p^2$	$1.93 \times 10^{15}$	$5.11 \times 10^{14}$	$2.36 \times 10^{13}$
Hollow - $2p$	$2.58 \times 10^{15}$	$6.77 \times 10^{14}$	$2.96 \times 10^{13}$
$2s2p^6$ - $2s2p^6$	$2.78 \times 10^{12}$	$1.14 \times 10^{14}$	$2.32 \times 10^{13}$
$2s2p^5$ - $2s2p^5$	$3.82 \times 10^{12}$	$1.49 \times 10^{14}$	$2.83 \times 10^{13}$
$2s2p^4$ - $2s2p^4$	$4.97 \times 10^{12}$	$1.85 \times 10^{14}$	$3.35 \times 10^{13}$
$2s2p^3$ - $2s2p^3$	$6.72 \times 10^{12}$	$2.21 \times 10^{14}$	$3.88 \times 10^{13}$
$2s2p^2$ - $2s2p^2$	$7.91 \times 10^{12}$	$2.57 \times 10^{14}$	$4.38 \times 10^{13}$
$2s2p$ - $2s2p^2$	$9.70 \times 10^{12}$	$2.94 \times 10^{14}$	$4.88 \times 10^{13}$
$2s$ - $2s^2$	$1.18 \times 10^{13}$	$3.28 \times 10^{14}$	$5.36 \times 10^{13}$
$2p^6$ - $2s2p^6$	$7.51 \times 10^{12}$	$3.21 \times 10^{14}$	$6.38 \times 10^{13}$
$2p^5$ - $2s2p^5$	$9.76 \times 10^{12}$	$3.97 \times 10^{14}$	$7.50 \times 10^{13}$
$2p^4$ - $2s2p^4$	$1.24 \times 10^{13}$	$4.75 \times 10^{14}$	$8.65 \times 10^{13}$
$2p^3$ - $2s2p^3$	$1.54 \times 10^{13}$	$5.48 \times 10^{14}$	$9.70 \times 10^{13}$
$2p^2$ - $2s2p^2$	$1.89 \times 10^{13}$	$6.22 \times 10^{14}$	$1.08 \times 10^{14}$
$2p$ - $2s2p$	$2.30 \times 10^{13}$	$6.92 \times 10^{14}$	$1.17 \times 10^{14}$
Hollow- $2s$	$2.78 \times 10^{13}$	$7.61 \times 10^{14}$	$1.27 \times 10^{14}$

decay rate via  $A_r$ ,  $A_a$ , and  $P_I$  processes in the  $k$ th state. The photon number ( $N_{hk}$ ) is given by

$$N_{hk} = \int_0^\infty P_k A_r dt. \quad (10)$$

Since we treat the x-ray emission with a single photon energy, we calculate  $N_{hk}$  emitted from the states of  $1s^22s^k2p^{k'}3s^23p^6$  ( $k=0$  or  $1$ ,  $k'=0 \sim 5$ ); Namely, we do not treat the x-ray emitted from the states in which a  $3s$  or  $3p$  electron is ionized.

We have employed approximations for the atomic data of the energy levels ( $E$ ),  $A_r$ , and  $A_a$  in order to avoid treating a large number of coupled rates. We should note that Suto and Kagawa have shown good agreement of their results calculated with this approximation with the experimental ones for spectroscopy from hollow atoms produced by the collision of argon ions with a solid [25]. The atomic data are averaged over the quantum numbers of spin angular momentum ( $S$ ), orbital angular momentum ( $L$ ), and total angular momentum ( $J$ ). The averaged transition energy ( $E_{av}$ ) and the averaged atomic data of  $A_a$  and  $A_r$  are given by

$$E_{av}(3s \rightarrow 2p) = \frac{\sum_{S,L,J} g_{SLJ} \sum_{S'L'J'} A_{rSLJS'L'J'} E_{SLJS'L'J'}}{\sum_{S,L,J} g_{SLJ} \sum_{S'L'J'} A_{rSLJS'L'J'}} \quad (11)$$

and

$$A_{av} = \frac{\sum_{S,L,J} g_{SLJ} A_{SLJ}}{\sum_{S,L,J} g_{SLJ}}, \quad (12)$$

respectively, where  $g_{SLJ}$  expresses the statistical weight of each state and the transition of  $A_{rSLJS'L'J'}$  and  $E_{SLJS'L'J'}$  is  $1s^22s^22p^53s^23p^6 \ ^S L_J \rightarrow 1s^22s^22p^63s3p^6 \ ^S L'_J$ . Table I lists  $E_{av}$ , and the rates for  $A_{r,av}$ , and  $A_{a,av}$  processes employed in our calculation.

### III. RESULTS AND DISCUSSIONS

Figure 2 shows the x-ray intensities for the original x-ray source and those from inner-shell excited states, doubly inner-shell excited states of  $2p$  electrons, and hollow atoms for  $n=2$  electrons of Ar as a function of time, where  $n$  is the principal quantum number. The irradiance, energy, and pulse of the original x-ray source are  $10^{14}$ – $10^{19}$  W/cm<sup>2</sup>, 1 keV, and 10 and 100 fs, respectively. We employ a Gaussian-type time function of the original x-ray source. In the case of the x-ray intensity of  $10^{14}$  W/cm<sup>2</sup> [see Figs. 2(a) and 2(d)], the x-ray pulse lengths emitted from doubly inner-shell excited states and hollow atoms become about 3/4 and 1/2 as short as that of the original x-ray source, respectively. On the other hand, for the fluorescence x-ray emitted from inner-shell excited states, the pulse length is almost the same. This comes from the fact that the production probabilities of the  $n$ th inner-shell excited states increase according to  $I^n$ , where  $I$  is the irradiance of the original x-ray source. As a result, the x-ray intensities emitted from inner-shell excited states are in proportion to those of the original x-ray source. On the other hand, multiply inner-shell excited states are produced only near the peak irradiance. For irradiances of  $10^{15}$ – $10^{17}$  W/cm<sup>2</sup>, we obtain almost the same results. For irradiances of more than  $10^{18}$  W/cm<sup>2</sup>, the pulse emitted from doubly inner-shell excited states and hollow atoms becomes much shorter [see Figs. 2(c) and 2(e)]: the pulse emitted from the hollow atoms becomes about 1/6 as short as that of the original source. This may come from the fact that the hollow atoms decay faster through the photoionization of the outer-shell electrons. When we employ multiply inner-shell excited states of  $d$  or  $f$  electrons of atoms with a larger atomic number, the pulse may be shorter because a larger number of  $n$  exist.

Figure 3 shows the ratio of the peak intensity of x-ray emissions from multiply inner-shell excited states and hollow atoms to that from inner-shell excited states of  $2p$  electrons as a function of  $I$ . We treat pulses of the original source of 10 and 100 fs in Figs. 3(a) and 3(b), respectively. It should be noted that the peak intensity of x-ray emissions from the inner-shell excited states of a  $2p$  electron is almost indepen-

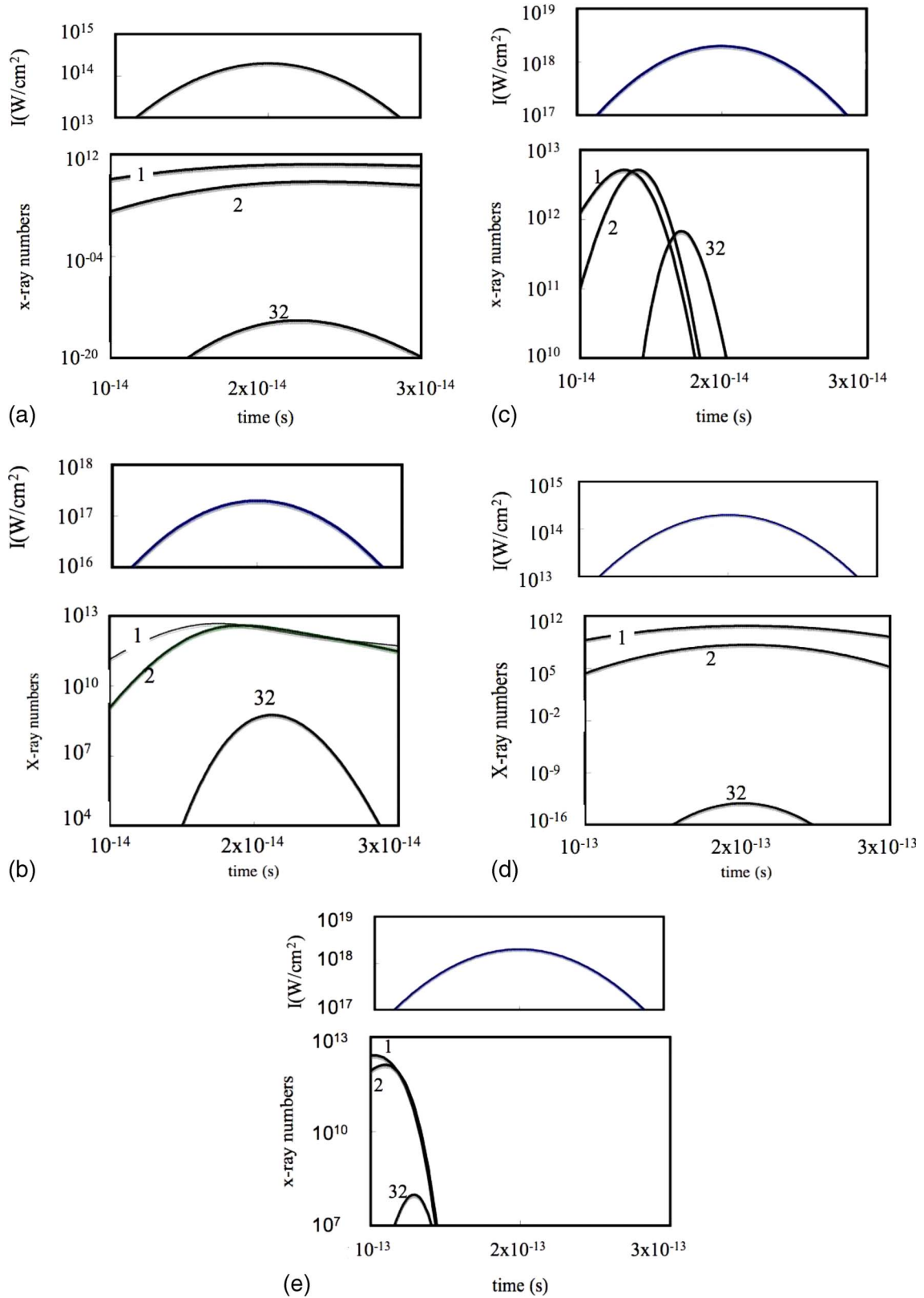


FIG. 2. (Color online) X-ray irradiance vs time for the original x-ray source (shown in the upper figure), x-ray emission from singly inner-shell excited states ( $1s^22s^22p^53s^23p^6$ ), doubly inner-shell excited states of  $2p$  electrons ( $1s^22s^22p^43s^23p^6$ ), and hollow atoms for  $n = 2$  states ( $1s^23s^23p^6$ ) using various x-ray intensities and x-ray pulses (shown in the lower figures). The intensity and pulses are (a)  $10^{14} \text{ W}/\text{cm}^2$ , 10 fs, (b)  $10^{17} \text{ W}/\text{cm}^2$ , 10 fs, (c)  $10^{18} \text{ W}/\text{cm}^2$ , 10 fs, (d)  $10^{14} \text{ W}/\text{cm}^2$ , 100 fs, and (e)  $10^{18} \text{ W}/\text{cm}^2$ , 100 fs. The numbers 1, 2, and 32 given in the figures correspond to the transitions  $1s^22s^22p^53s^23p^6 \rightarrow 1s^22s^22p^63s3p^6$ ,  $1s^22s^22p^43s^23p^6 \rightarrow 1s^22s^22p^53s3p^6$ , and  $1s^23s^23p^6 \rightarrow 1s^22s3s^23p^5$  as listed in Table I(a), respectively.

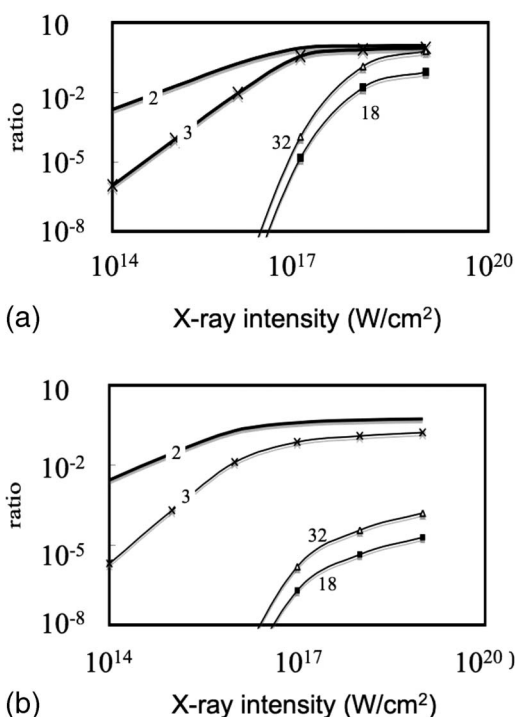


FIG. 3. Ratio of x-ray irradiance emitted from doubly inner-shell excited states of  $2p$  electrons ( $1s^2 2s^2 2p^4 3s^2 3p^6$ ), and hollow atoms for  $n=2$  states ( $1s^2 3s^2 3p^6$ ). The numbers 2, 3, 18, and 32 given in the figures correspond to the transitions  $1s^2 2s^2 2p^4 3s^2 3p^6 \rightarrow 1s^2 2s^2 2p^5 3s 3p^6$ ,  $1s^2 2s^2 2p^3 3s^2 3p^6 \rightarrow 1s^2 2s^2 2p^4 3s 3p^6$ ,  $1s^2 3s^2 3p^6 \rightarrow 1s^2 2p 3s 3p^6$ , and  $1s^2 3s^2 3p^6 \rightarrow 1s^2 2s 3s^2 3p^5$  as listed in Table I(a). The pulses are (a) 10 and (b) 100 fs.

dent of the pulses and intensities of the original x-ray source for intensities of more than  $10^{16}$  W/cm<sup>2</sup>. Therefore, the rates in Figs. 3 are the creation rates of multiply inner-shell excited states and hollow atoms. For x-ray emission from the doubly and triply excited states, the x-ray emission is almost the same as that from the inner-shell excited states, and saturates around  $I \sim 10^{16}$  W/cm<sup>2</sup>. For the 100 fs pulse, the ratio for the hollow atoms is as small as  $10^{-4}$  even for an irradi-

ance of more than  $10^{18}$  W/cm<sup>2</sup> [see Fig. 3(b)]. On the other hand, for the 10 fs pulse, the ratio becomes about 0.5 at the irradiance of  $10^{19}$  W/cm<sup>2</sup> [see Fig. 3(a)]. This may come from the fact that the hollow atoms are produced at a higher x-ray intensity for the 10 fs pulse than for the 100 fs pulse because the hollow atoms are produced before the peak x-ray intensity. The effect of the production of an  $n$  times inner-shell excited state from an  $n-1$  times inner-shell excited state is governed by the following branching ratio:

$$\frac{\beta_n}{\alpha_{n-1,n} + \beta_n}, \quad (13)$$

where  $\alpha_{n-1}$  is almost determined by the rate of autoionization and  $\beta_n$  is the rate of inner-shell ionization. That is, higher intensities of x rays, which produce larger  $\beta_n$  values [21], result in more efficient production of the hollow atoms.

#### IV. SUMMARY

We study the time dependence of multiply inner-shell excited states produced by high-brightness x rays and of the x-ray emission processes from these multiply inner-shell excited states. We have found that the x-ray pulse emitted from multiply inner-shell excited states may become shorter than the pulse of the original x-ray sources. When the x-ray irradiance becomes more than  $10^{18}$  W/cm<sup>2</sup>, the pulse becomes about one-sixth the size of that of the original x-ray source; namely, higher intensities of x rays result in a more efficient production of hollow atoms. We have found that hollow atoms are produced more efficiently as the pulse of x-ray sources decreases.

#### ACKNOWLEDGMENTS

We wish to thank Professor T. Tajima, Professor K. Nami-kawa, Professor N. Go, Professor T. Kagawa, Professor D.E. Kim, M. Ishino, Dr. Y. Fukuda, Dr. T. Imazono, Dr. H. Kono, Dr. A. Matsumoto, Dr. J. Koga, Dr. M. Yamagiwa, and Dr. T. Kimura for useful discussions. We use Cowan's code for the calculations of atomic data.

[1] See <http://xfel.desy.de/> for the European x-ray laser project XFEL and <http://www-ssrl.slac.stanford.edu/lcls/> for the LCLS project.  
 [2] D. Normile, *Science* **314**, 751 (2006).  
 [3] T. Pfeifer, C. Spielmann, and G. Gerber, *Rep. Prog. Phys.* **69**, 443 (2006).  
 [4] Y. Ueshima, Y. Kishimoto, A. Sasaki, and T. Tajima, *Laser Part. Beams* **17**, 45 (1999).  
 [5] Y. Nabekawa, H. Hasegawa, E. J. Takahashi, and K. Midorikawa, *Phys. Rev. Lett.* **94**, 043001 (2005).  
 [6] K. Lee, Y. H. Cha, M. S. Shin, B. H. Kim, and D. Kim, *Opt. Express* **11**, 309 (2003).  
 [7] A. Zhidkov, J. Koga, A. Sasaki, and M. Uesaka, *Phys. Rev. Lett.* **88**, 185002 (2002).  
 [8] R. Neutze, R. Wouts, D. van der Spoel, E. Weckert, and J.

Hajdu, *Nature (London)* **406**, 752 (2000).  
 [9] S. P. Hau-Riege, R. A. London, and A. Szoke, *Phys. Rev. E* **69**, 051906 (2004).  
 [10] M. Bargheer, N. Zhavoronkov, M. Woerner, and T. Elsaesser, *ChemPhysChem* **7**, 793 (2006).  
 [11] T. Guo, C. R. Petruck, R. Jimenez, F. Ràksi, J. Squier, B. Walker, K. R. Wilson, and C. P. J. Barty, *Proc. SPIE* **3157**, 84 (1997).  
 [12] H. Kandori, H. Sasabe, K. Nakanishi, T. Yoshizawa, T. Mizukami, and Y. Shichida, *J. Am. Chem. Soc.* **118**, 320 (1996).  
 [13] M. Yan, L. Rothberg, and R. Callender, *J. Phys. Chem.* **105**, 856 (2001).  
 [14] S. Akimoto, S. Takaichi, T. Ogata, Y. Nishimura, I. Yamazaki, and M. Mimuro, *Chem. Phys. Lett.* **260**, 147 (1996).  
 [15] D. Polli, G. Cerullo, G. Lanzani, S. D. Silvestri, H. Jashimoto,

- and R. J. Cogdell, *Biophys. J.* **90**, 2486 (2006).
- [16] F. Paerels, J. Cottam, M. Sako, D. A. Liedahl, A. C. Brinkman, R. L. J. van der Meer, J. S. Kaastra, and P. Predehl, *Astrophys. J.* **553**, L135 (2000).
- [17] D. A. Liedahl and F. Paerels, *Astrophys. J.* **468**, L33 (1996).
- [18] *Auger Electron Spectroscopy*, edited by C. L. Briant and R. P. Messmer *Treatise on Materials Science and Technology*, Vol. 30 (Academic Press, New York, 1988).
- [19] M. Tegze and G. Faigel, *Nature (London)* **380**, 49 (1996).
- [20] K. Hayashi, T. Hayashi, Y. Takahashi, S. Suzuki, and E. Matsubara, *Nucl. Instrum. Methods Phys. Res. B* **238**, 192 (2005).
- [21] K. Moribayashi, A. Sasaki, and T. Tajima, *Phys. Rev. A* **58**, 2007 (1998).
- [22] K. Moribayashi, T. Kagawa, and D. E. Kim, *J. Phys. B* **37**, 4119 (2004).
- [23] K. Moribayashi, T. Kagawa, and D. E. Kim, *J. Phys. B* **38**, 2187 (2005).
- [24] R. D. Cowan, *J. Opt. Soc. Am.* **58**, 808 (1968).
- [25] K. Suto and T. Kagawa, *Phys. Rev. A* **58**, 5004 (1998); **63**, 019903(E) (2000).